

Visualizing departures from marginal homogeneity for square contingency tables with ordered categories

Satoru Shinoda¹, Takuya Yoshimoto² and Kouji Tahata³

¹*Department of Biostatistics, Yokohama City University, School of Medicine, Japan*

²*Biometrics Department, Chugai Pharmaceutical Co., Ltd., Japan*

³*Department of Information Sciences, Faculty of Science and Technology, Tokyo University of Science, Japan*

E-mail: shinoda.sat.cg@yokohama-cu.ac.jp

Abstract

Square contingency tables are a special case commonly used in various fields to analyze categorical data. Although several analysis methods have been developed to examine marginal homogeneity (MH) in these tables, existing measures are single-summary ones. To date, a visualization approach has yet to be proposed to intuitively depict the results of MH analysis. Current measures used to assess the degree of departure from MH are based on entropy such as the Kullback-Leibler divergence and do not satisfy distance postulates. Hence, the current measures are not conducive to visualization. Herein we present a measure utilizing the Matusita distance and introduce a visualization technique that employs sub-measures of categorical data. Through multiple examples, we demonstrate the meaningfulness of our visualization approach and validate its usefulness to provide insightful interpretations.

Key words: Marginal homogeneity, Matusita distance, power-divergence, visualization.

1. Introduction

Numerous research areas employ categorical data analysis. Such data is summarized in a contingency table (see e.g., Agresti, 2013; Kateri, 2014). A special case is a square contingency table where the row and column variables have the same ordinal categories. When we cannot obtain data as continuous variables for the evaluation of the efficacy and safety/toxicity of treatments in clinical studies, ordered categorical scales are used alternatively.

For example, Sugano *et al.* (2012) conducted a clinical study where they examined the modified LANZA score (MLS) after 24 weeks' treatment with esomeprazole 20 mg once daily or a placebo. The MLS is a popular evaluation scale with five stages (from 0 to +4) and is used for clinical evaluations of gastroduodenal mucosal lesions. Table 1 shows a square contingency table that summarizes the location shift of the MLS from pre-treatment to post-treatment for each patient. Such research is interested in whether the treatment effect tends to improve or worsen after an intervention relative to before the intervention. Thus, the evaluation is interested in the similarity from marginal homogeneity (MH), but not independence. Stuart (1955) introduced the MH model to indicate homogeneity with respect to two marginal distributions. We are also interested in the structure of inhomogeneity of the two marginal distributions when the MH model does not hold. This is because we are more interested in the deviation between the pre-treatment and post-treatment marginal distributions (i.e., intervention results) than whether the MH model that represents the structure shows an equal marginal distribution for the data in Table 1. Consequently, our strategy is to estimate measures representing the degree of departure from MH. Measures must quantify the differences in probability distributions, mainly using information divergences such as Kullback-Leibler divergence or power-divergence.

To this end, Tomizawa, Miyamoto and Ashihara (2003) proposed a measure using the marginal cumulative probability for square contingency tables with ordered categories. This measure ranges from 0 to 1 and directly rep-

Table 1: Shift analysis data of MLS after treatment for 24 weeks with esomeprazole 20 mg once daily or a placebo.

Study end	Baseline				
	0	+1	+2	+3	+4
(a) Esomeprazole 20 mg once daily					
0	78	9	26	3	1
+1	1	5	6	4	0
+2	9	1	10	3	1
+3	1	0	1	0	0
+4	3	0	1	1	2
(b) Placebo					
0	41	2	19	0	0
+1	8	0	4	0	0
+2	12	4	14	3	0
+3	0	1	1	3	0
+4	29	7	11	6	0

resents the degree of departure from MH. However, it cannot distinguish the direction of degree of departure. The two marginal distributions are interpreted as equal (no intervention effect) when the value is 0. When the values are greater than 0, an improvement is indistinguishable from a worsening effect. Yamamoto, Ando and Tomizawa (2011) proposed a measure, which lies between -1 and 1, to distinguish the directionality. This measure cannot represent the degree of departure directly from MH. Even if the value of the measure is 0, the marginal distribution cannot be exactly interpreted as having no intervention effect. To simultaneously analyze the degree and directionality of departure from MH, Ando, Noguchi, Ishii and Tomizawa (2021) proposed a two-dimensional visualized measure that combines the measure proposed by Tomizawa *et al.* (2003) and the measure proposed by Yamamoto *et al.* (2011). They also considered visually comparing the degrees of departure from MH in several tables because their measure is independent of the dimensions (i.e., number of categorical values) and sample size. Appendix 1 explains the main points of the above measures.

These measures proposed by Tomizawa *et al.* (2003), Yamamoto *et al.*

(2011) and Ando *et al.* (2021) are single-summaries. They are expressed using the sub-measure weights at each categorical level. For a given category level, different behaviors cannot be distinguished as a single-summary measure. The artificial data examples in the data analysis section provide specific situations. Hence, a single-summary-measure may overlook different behaviors in a given categorical level. To address this limitation, we apply visualization as a method utilizing sub-measures defined at each category level. This visualization also assumes that satisfying distance postulates can achieve a natural interpretation. To date, a measure for ordered categories does not exist because the Kullback-Leibler divergence or power-divergence used in existing measures do not satisfy the distance postulates. Therefore, we consider a measure using the Matusita distance to capture the discrepancy between two probability distributions while satisfying the distance postulates (see Matusita, 1954, 1955; Read and Cressie, 1988, p.112).

Both academia and general society employ methods to visualize quantitative data. Examples include pie charts, histograms, and scatterplots. Although visualizing categorical data has attracted attention recently, different visualization techniques from those for quantitative data are necessary (see, e.g., Blasius and Greenacre, 1998; Friendly and Meyer, 2015; Kateri, 2014). Visualization of categorical data has two main objectives: revealing the characteristics of the data and intuitively understanding analysis results (Friendly and Meyer, 2015). Methods for the former include the “mosaic plot” and “sieve diagram” (see e.g., Friendly, 1995; Hartigan and Kleiner, 1981, 1984; Riedwyl and Schüpbach, 1983, 1994). Methods for the latter include the “fourfold display” for odds ratios and the “observer agreement chart” for Cohen’s κ (see e.g., Bangdiwala 1985, 1987; Fienberg, 1975; Friendly, 1994). Although the visualization objectives for categorical data may vary, they share common techniques: (i) separating data by categorical levels and (ii) adjusting the size of figure objects based on the frequency of each cell.

Our research aims to realize a visualization for an intuitive understanding

of the analysis results for MH. To date, such a visualization has yet to be proposed. Although the “mosaic plot” and “sieve diagram” can be applied to square contingency tables, they are not suitable for examining the structure of MH. These visualizations are designed to observe the data itself and identify features or patterns without making hypotheses before analyzing the data. Therefore, our proposed visualization provides an intuitive understanding of the structure of MH using categorical data visualization techniques (i) and (ii).

This paper conducts a comprehensive analysis of the degree and directionality of departure from MH for square contingency tables with ordered categories. Our approach has two components: (i) measures to quantify the degree of departure of MH using information divergence satisfying distance postulates and (ii) a visualization technique designed for categorical data.

The rest of this paper is organized as follows. Section 2 defines the proposed measure and visualization. Section 3 derives an approximated confidence interval for the proposed measure. Section 4 provides examples of the utility for the proposed measure and visualization. Section 5 presents the discussion. Finally, Section 6 closes with concluding remarks.

2. Proposed measure and visualization

Here, we detail the proposed measure and visualization. Section 2.1 explains the probability structure of the MH model using formulas. Section 2.2 defines the sub-measures and single-summary-measure expressed using weights for the sub-measures at each categorical level along with the properties of the proposed measure. Section 2.3 details the visualization of the proposed measures.

2.1. MH model

Consider an $r \times r$ square contingency table with the same row and column ordinal classifications. Let X and Y denote the row and column variables, respectively, and let $\Pr(X = i, Y = j) = p_{ij}$ for $i = 1, \dots, r; j = 1, \dots, r$.

The MH model can be expressed with various formulas. For example, the MH model is expressed as

$$p_{i\cdot} = p_{\cdot i} \quad \text{for } i = 1, \dots, r,$$

where $p_{i\cdot} = \sum_{t=1}^r p_{it}$ and $p_{\cdot i} = \sum_{s=1}^r p_{si}$. See e.g., Stuart (1955) and Bishop, Fienberg and Holland (1975, p.294). This indicates that the row marginal distribution is identical to the column marginal distribution.

To consider ordered categories, the MH model can be expressed using the marginal cumulative probability as

$$F_{1(i)} = F_{2(i)} \quad \text{for } i = 1, \dots, r - 1,$$

where $F_{1(i)} = \sum_{s=1}^i p_{s\cdot} = \Pr(X \leq i)$ and $F_{2(i)} = \sum_{t=1}^i p_{\cdot t} = \Pr(Y \leq i)$. The MH model can also be expressed as

$$G_{1(i)} = G_{2(i)} \quad \text{for } i = 1, \dots, r - 1,$$

where $G_{1(i)} = \sum_{s=1}^i \sum_{t=i+1}^r p_{st} = \Pr(X \leq i, Y \geq i+1)$ and $G_{2(i)} = \sum_{s=i+1}^r \sum_{t=1}^i p_{st} = \Pr(X \geq i+1, Y \leq i)$. Furthermore, the MH model can be expressed as

$$G_{1(i)}^c = G_{2(i)}^c \left(= \frac{1}{2} \right) \quad \text{for } i = 1, \dots, r - 1,$$

where

$$G_{1(i)}^c = \frac{G_{1(i)}}{G_{1(i)} + G_{2(i)}}, \quad G_{2(i)}^c = \frac{G_{2(i)}}{G_{1(i)} + G_{2(i)}}.$$

The MH model states that the conditional probability of $X \leq i$ is given if either X or $Y \leq i$ and the other $\geq i+1$ is equal to the conditional probability that $Y \leq i$ for the same conditions.

2.2. Measure of departure from MH

Several measures have been proposed for various formulas of the MH model. Here, we consider a measure that is independent of the diagonal

probabilities because the MH model does not have constraints on the main-diagonal cell probabilities. For instance, Tomizawa *et al.* (2003) and Yamamoto *et al.* (2011) proposed measures that do not depend on the diagonal probabilities.

First, we consider a sub-measure satisfying the distance postulates. Assuming that $G_{1(i)} + G_{2(i)} \neq 0$, the degree of departure from MH at each categorical level i ($i = 1, \dots, r - 1$) is given as

$$\gamma_i = \left[\frac{2 + \sqrt{2}}{2} (v_{1(i)}^2 + v_{2(i)}^2) \right]^{\frac{1}{2}},$$

where

$$v_{1(i)} = \sqrt{G_{1(i)}^c} - \sqrt{\frac{1}{2}}, \quad v_{2(i)} = \sqrt{G_{2(i)}^c} - \sqrt{\frac{1}{2}}.$$

The sub-measure γ_i has the following characteristics:

- (i) $0 \leq \gamma_i \leq 1$
- (ii) $\gamma_i = 0$ if and only if $G_{1(i)}^c = G_{2(i)}^c (= 1/2)$
- (iii) $\gamma_i = 1$ if and only if $G_{1(i)}^c = 1$ (then $G_{2(i)}^c = 0$) or $G_{1(i)}^c = 0$ (then $G_{2(i)}^c = 1$)

The sub-measure γ_i is the Matusita distance between $(G_{1(i)}^c, G_{2(i)}^c)$ and $(\frac{1}{2}, \frac{1}{2})$, and satisfies all three distance postulates. When the value of the sub-measure is 0, it means the marginal cumulative probabilities are equivalent until categorical level i . The value of the sub-measure increases as the separation between the marginal cumulative distributions increases. The separation is maximized when the value of the sub-measure is 1. Noting that a distance d is defined on a set W if for any two elements $x, y \in W$, a real number $d(x, y)$ is assigned that satisfies the following postulates:

- (i) $d(x, y) \geq 0$ with equality if and only if $x = y$;
- (ii) $d(y, x) = d(x, y)$;

(iii) $d(x, z) \leq d(x, y) + d(y, z)$ for $x, y, z \in W$ (the triangle inequality).

See also Read and Cressie (1988, p.111). Then the power-divergence $I^{(\lambda)}$ (especially, the Kullback-Leibler divergence $I^{(0)}$) does not satisfy postulates (ii) and (iii). The Matusita distance, which is the square root of $I^{(-\frac{1}{2})}$, satisfies all three postulates.

Assuming that $\{G_{1(i)} + G_{2(i)} \neq 0\}$, we consider a measure using sub-measure γ_i to represent the degree of departure from MH, which is given as

$$\Gamma = \sum_{i=1}^{r-1} (G_{1(i)}^* + G_{2(i)}^*) \gamma_i,$$

where

$$\Delta = \sum_{i=1}^{R-1} (G_{1(i)} + G_{2(i)}),$$

and

$$G_{1(i)}^* = \frac{G_{1(i)}}{\Delta}, \quad G_{2(i)}^* = \frac{G_{2(i)}}{\Delta},$$

for $i = 1, \dots, r - 1$. The measure Γ has the following characteristics:

- (i) $0 \leq \Gamma \leq 1$
- (ii) $\Gamma = 0$ if and only if the MH model holds
- (iii) $\Gamma = 1$ if and only if the degree of departure from MH is a maximum, in the sense that $G_{1(i)}^c = 1$ (then $G_{2(i)}^c = 0$) or $G_{1(i)}^c = 0$ (then $G_{2(i)}^c = 1$), for $i = 1, \dots, r - 1$

Thus, this measure is the weighted sum of the Matusita distance for the two distributions $(G_{1(i)}^c, G_{2(i)}^c)$ and $(\frac{1}{2}, \frac{1}{2})$.

2.3. Visualization of the proposed measure

To visualize the proposed measure, we used the techniques for visualizing categorical data. First, for the fixed i ($i = 1, \dots, r - 1$), γ_i , which represents the relationship between $G_{1(i)}^c$ and $G_{2(i)}^c$, is defined by the following steps:

- (i) Plot the x -axis is $G_{1(i)}^c$ and the y -axis is $G_{2(i)}^c$ point for each $(G_{1(i)}^c, G_{2(i)}^c)$ coordinate
- (ii) Adjust the point size according to the weight $(G_{1(i)}^* + G_{2(i)}^*)$
- (iii) Display the value of γ_i as a text label at each $(G_{1(i)}^c, G_{2(i)}^c)$ point
- (iv) Color the points red when $(G_{1(i)}^c < G_{2(i)}^c)$ and blue when $(G_{1(i)}^c \geq G_{2(i)}^c)$
- (v) Draw the dashed line within the diagonal point's range of movement and color the dashed line using the same rules

Therefore, the top-left side is red, while the bottom-right side is blue with respect to the point $(\frac{1}{2}, \frac{1}{2})$ in the visualization. Table 2 shows a visualization image. Table 3 presents the necessary information to visualize Table 2, in-

Table 2: True cell probabilities in a 6×6 square contingency table.

	1	2	3	4	5	6
1	0.000	0.031	0.219	0.031	0.031	0.000
2	0.000	0.000	0.031	0.031	0.031	0.000
3	0.000	0.031	0.000	0.031	0.031	0.000
4	0.000	0.031	0.031	0.000	0.031	0.000
5	0.000	0.031	0.031	0.031	0.000	0.000
6	0.000	0.031	0.031	0.219	0.031	0.000

cluding $G_{1(i)}^c$ and $G_{2(i)}^c$ used for the coordinates of the point, the weight used for the point size, and the sub-measure γ_i used for the text label. Step 1

Table 3: Visualization values of γ_i .

i	x -axis	y -axis	size	label
1	1.000	0.000	0.156	1.000
2	0.750	0.250	0.250	0.341
3	0.500	0.500	0.188	0.000
4	0.250	0.750	0.250	0.341
5	0.000	1.000	0.156	1.000

visualizes each level i . As an example, Figure 1 depicts how γ_i is visualized at level $i = 1$.

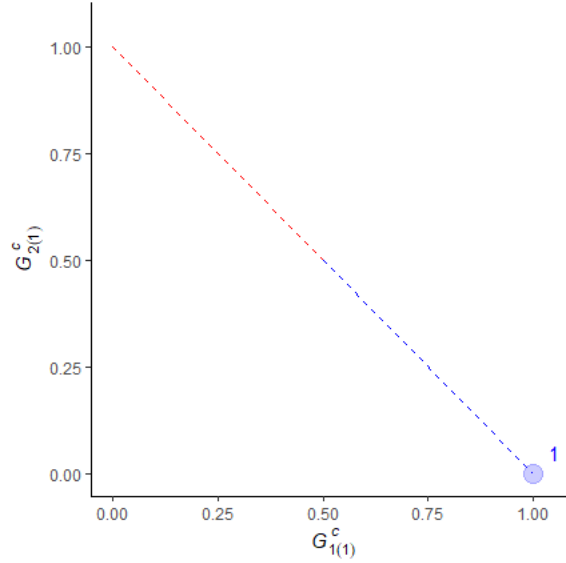


Figure 1: Visualization of γ_1 .

Next, we provide additional definitions to integrate each γ_i in step 1 into one figure:

- (i) Consider the x -axis as i for $G_{1(i)}^c$ and the y -axis as i for $G_{2(i)}^c$
- (ii) Place the figure of γ_i on the diagonal

Figure 2 shows the integrated figure using the example from Table 2 in step 2 according to the definition of the proposed visualization.

The visualization of the proposed measure using the categorical data methods has the following benefits. First, the visualization provides information about each i , allowing trends in MH to be identified in a square contingency table. Since the figure visualizes each γ_i , points do not overlap even if their coordinates are close. Thus, points are easily identifiable. It is important to visualize each γ_i separately since each one is assumed to be nearly the same value.

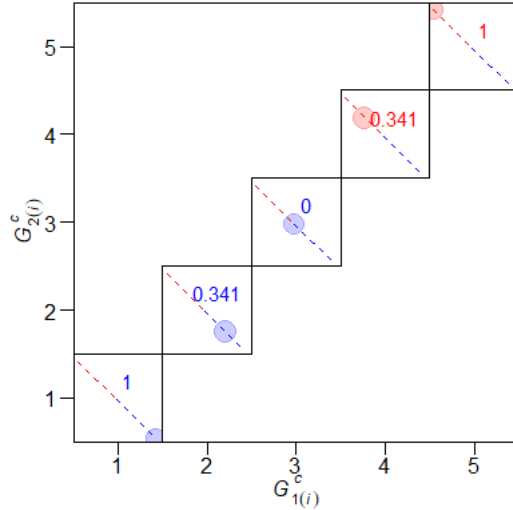


Figure 2: Proposed visualization to provide an intuitive understanding of the structure of MH

Ando *et al.* (2021) used a Kullback-Leibler divergence-type measure, but the Kullback-Leibler divergence does not satisfy the distance postulates. To naturally interpret the point distances in the figure, the distance postulates must be satisfied. (Section 4.1.1. gives a specific example). Additionally, the proposed visualization can be considered as utilizing sub-measures.

3. Approximate the confidence interval for the measure

Let n_{ij} denote the observed frequency in the i th row and j th column of a table ($i = 1, \dots, r; j = 1, \dots, r$). The sample version of Γ (i.e., $\hat{\Gamma}$) is given by Γ in which $\{p_{ij}\}$ is replaced by $\{\hat{p}_{ij}\}$, where $\hat{p}_{ij} = n_{ij}/n$ and $n = \sum \sum n_{ij}$. It should be noted that the sample version of $G_{k(i)}^c$, γ_i and $F_{k(i)}$, which are $\hat{G}_{k(i)}^c$, $\hat{\gamma}_i$ and $\hat{F}_{k(i)}$, respectively, are given in a similar manner ($i = 1, \dots, r - 1; k = 1, 2$). Given that $\{n_{ij}\}$ arises from a full multinomial sampling, we can estimate the standard error for $\hat{\Gamma}$ and construct a large-sample confidence interval for Γ . The delta method can approximate the

standard error. $\sqrt{n}(\hat{\Gamma} - \Gamma)$ has an asymptotic (as $n \rightarrow \infty$) normal distribution with mean zero and variance $\sigma^2[\Gamma]$. See Appendix 2 for the details of $\sigma^2[\Gamma]$.

Let $\hat{\sigma}^2[\Gamma]$ denote $\sigma^2[\Gamma]$ where $\{p_{ij}\}$ is replaced by $\{\hat{p}_{ij}\}$. Then $\hat{\sigma}[\Gamma]/\sqrt{n}$ is the estimated approximate standard error for $\hat{\Gamma}$, and $\hat{\Gamma} \pm z_{p/2}\hat{\sigma}[\Gamma]/\sqrt{n}$ is an approximate $100(1 - p)$ percent confidence interval for Γ , where $z_{p/2}$ is the $100(1 - p/2)$ th percentile of the standard normal distribution.

The asymptotic normal distribution may not be applicable when estimating measures on small sample datasets. In small dataset, the sample proportion of (i, j) cell may fall 0 (i.e., $\hat{p}_{ij} = 0$). Thus, we consider Bayesian methods. Although the sample proportion is typically used to estimate the approximate standard error for $\hat{\Gamma}$, herein we consider the Bayes estimator derived from the uninformed prior probability. To have a vague prior, the Haldane prior is used for the prior information (see Haldane 1932; Berger 1985, p.89). We set all parameters of the Dirichlet distribution to 0.0001 when estimating the approximate variance of the proposed measure.

4. Data analysis

4.1. Artificial data

4.1.1. Role of distance postulates for visualization

To illustrate the concept of visualization, we used artificial datasets in two scenarios: one that satisfies the structure of MH and one that has location-shifted marginal distributions.

The visualization in Table 4(a) shows that all values of sub-measure $\hat{\gamma}_i$ are equal to zero, and the value of the proposed measure $\hat{\Gamma}$ is zero (i.e., the MH model holds). In terms of information divergences, the two marginal distributions can be interpreted as the same. Therefore, the values of the label, which is the sub-measure using the Matusita distance, are zero, and points are drawn at $(\frac{1}{2}, \frac{1}{2})$ in the visualization (Figure 3(a)).

The visualization in Table 4(b) shows that all values of sub-measure $\hat{\gamma}_i$ are equal to 0.341 because the assumed structure shows location-shifted marginal distributions. Since we estimated $(\hat{G}_{1(i)}^c < \hat{G}_{2(i)}^c)$, the point on the graph is

drawn from $(\frac{1}{2}, \frac{1}{2})$ to the upper left (Figure 3(b)). Because the label values are sub-measures using the Matusita distance that satisfies distance postulate (ii), it can be interpreted as the distance between $(G_{1(i)}^c, G_{2(i)}^c)$ and $(\frac{1}{2}, \frac{1}{2})$. However, the direction is crucial when using the Kullback-Leibler divergence (see Appendix 1). When using the Kullback-Leibler divergence in Table 4(b), the distance from $(\frac{1}{2}, \frac{1}{2})$ to $(G_{1(i)}^c, G_{2(i)}^c)$ and the distance from $(G_{1(i)}^c, G_{2(i)}^c)$ to $(\frac{1}{2}, \frac{1}{2})$ differ (Table 5). Therefore, the label value must be selected carefully because this divergence may hinder an intuitive interpretation. In addition, it can be evaluated appropriately in indirect comparisons between two points for the distance from a reference since the proposed measure satisfies the triangular inequalities.

Thus, the visualization must use a divergence that satisfies the distance postulates. In addition, the proposed visualization gives a natural and intuitive interpretation because we can understand the degree of departure from MH for each level i , and the sub-measure calculated by $\hat{G}_{1(i)}^c$ and $\hat{G}_{2(i)}^c$ compares the marginal cumulative distributions $(\hat{F}_{1(i)}$ and $\hat{F}_{2(i)})$. This section shows the visualization in monotonic differences of the marginal cumulative distributions, but the next section illustrates the relationship between marginal cumulative distributions and visualizations in several patterns.

Table 4: Artificial data.

	1	2	3	4
(a)				
1	0	10	10	10
2	10	0	10	10
3	10	10	0	10
4	10	10	10	0
(b)				
1	0	10	10	10
2	30	0	10	10
3	30	30	0	10
4	30	30	30	0

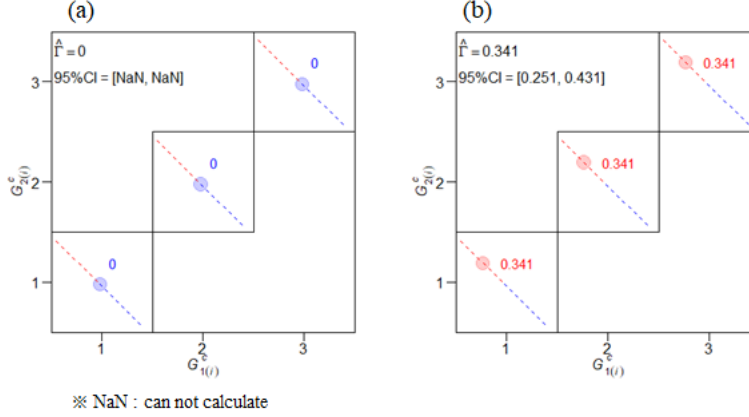


Figure 3: Visualization result of Table 4.

Table 5: Values of the Kullback-Leibler divergence.

i	$\hat{G}_{1(i)}^c$	$\hat{G}_{2(i)}^c$	\hat{K}_i^1	\hat{K}_i^2
1	0.250	0.750	0.131	0.144
2	0.250	0.750	0.131	0.144
3	0.250	0.750	0.131	0.144

$$\hat{K}_i^1 = I_i^{(0)} \left(\left\{ \hat{G}_{1(i)}^c, \hat{G}_{2(i)}^c \right\}; \left\{ \frac{1}{2}, \frac{1}{2} \right\} \right)$$

$$\hat{K}_i^2 = I_i^{(0)} \left(\left\{ \frac{1}{2}, \frac{1}{2} \right\}; \left\{ \hat{G}_{1(i)}^c, \hat{G}_{2(i)}^c \right\} \right)$$

4.1.2. Perception of different behaviors between categorical levels

Our visualization can interpret the relationships between the marginal cumulative distributions, which is difficult using a single-summary-measure. Here, we treat artificial data where the values of the single-summary-measure are the same, but the visualizations of the sub-measures behave differently. Tables 6(a)–(d) show the artificial data, which are setup so that the value of the measure is 0.341. Figures 4(a)–(d) show the visualizations of Tables 6(a)–(d).

Table 6(a) illustrates a scenario where the marginal cumulative distribution is location-shifted constantly. This structure would be expected based on the value of the measure. In a clinical study, assuming such a situation

implies a constant treatment effect from pre-treatment to post-treatment.

In contrast, Table 6(b) represents a scenario where the marginal cumulative distribution spreads as the categorical level i increases. Moreover, Tables 6(c)–(d) show situations where the marginal cumulative distribution differs at the categorical level i . In a clinical study, assuming such a situation suggests that the treatment effect depends on the pre-intervention condition.

Table 6: Artificial data.

	1	2	3	4
(a)				
1	0	30	30	30
2	10	0	30	30
3	10	10	0	30
4	10	10	10	0
(b)				
1	0	5	5	6
2	5	0	11	36
3	5	10	0	86
4	5	10	10	0
(c)				
1	0	30	30	30
2	10	0	0	30
3	10	240	0	30
4	10	10	10	0
(d)				
1	0	30	30	30
2	10	0	30	30
3	10	10	0	0
4	10	10	160	0

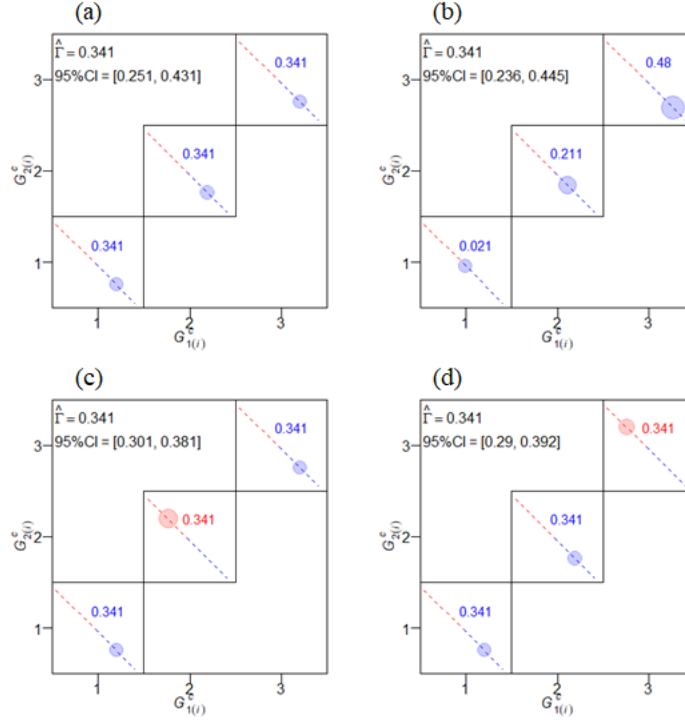


Figure 4: Visualization result of Table 6.

4.2. Simulation studies

Monte Carlo simulations were performed to theoretically derive the coverage probabilities of the approximate 95% confidence intervals assuming random sampling of an underlying bivariate normal distribution. Here, we considered random variables Z_1 and Z_2 with means $E(Z_1) = 0$ and $E(Z_2) = d$, variances $\text{Var}(Z_1) = \text{Var}(Z_2) = 1$, and correlation $\text{Corr}(Z_1, Z_2) = 0.2$. Assuming a 6×6 table is formed using the cutoff points for each variable at $-1.2, -0.6, 0, 0.6, 1.2$, we evaluated several simulation scenarios where $d = 0.00$ to 4.00 by 0.25 and $n = 36, 180, 360, 3600$ (sparseness index = $1, 5, 10, 100$). The simulation studies were performed based on 100,000 trials per scenario.

Figure 5 plots the mean of random variable Z_2 along with the true value of the measure based on a bivariate normal distribution. When $d = 0$, the

true value of the measure is observed as 0 because there is no difference in the means whose condition is stronger than the structure of the MH. Although the true value increases monotonically for $d = 0, \dots, 1$, a large mean difference between random variables is necessary for the true value to reach 1.

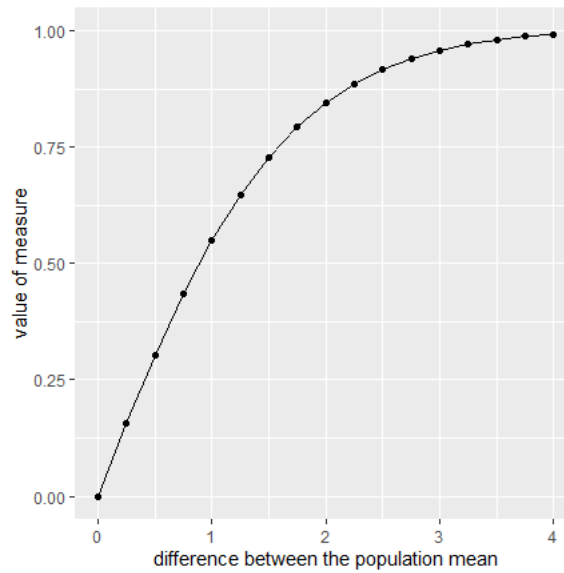


Figure 5: Mean of random variable Z_2 and the true value of the measure, which are based on a bivariate normal distribution.

Figure 6 shows the coverage probability according to the true values. For a small sample size, it is difficult to obtain a nominal coverage probability, whereas the coverage probability is maintained at a 95% confidence interval for a sufficient sample size.

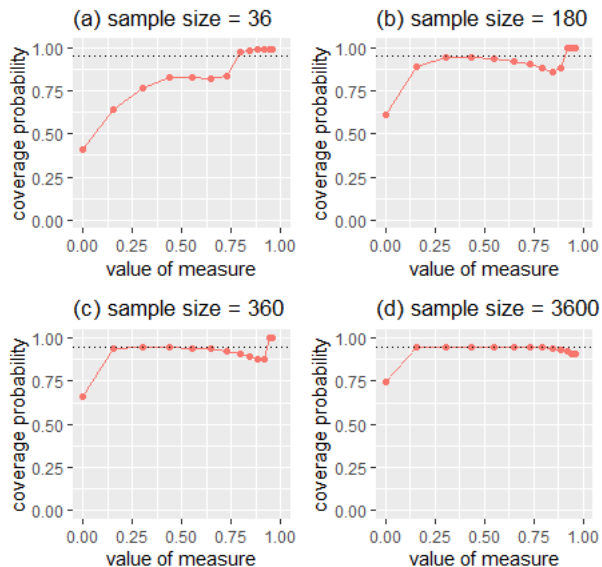


Figure 6: Transitions of true values and coverage probabilities.

4.3. Example

As an example, consider the data in Table 1. In the original work (Sugano *et al.*, 2012), the proportion of improvement or deterioration for the esomeprazole group (drug group) and placebo group were described. Table 7 shows the results of applying the proposed measure Γ to these data to statistically consider the treatment effects for the drug or placebo. The estimate of asymptotic variance using the sample proportion cannot be calculated because $\hat{G}_{1(4)}^c = 0$ in Table 1(b). Hence, a Bayes estimator is used to estimate the asymptotic variance. The 95% confidence intervals do not cross zero, suggesting that both groups have a higher degree of deviation from MH. That is, the marginal distribution after the treatment shifts compared to that before the treatment.

For an intuitive understanding, Figure 7 plots the trend, where blue indicates an improving trend and red a deteriorating one. The drug group shows an improving trend ($\hat{G}_{1(i)}^c \geq \hat{G}_{2(i)}^c$), while the placebo group displays a deteriorating trend ($\hat{G}_{1(i)}^c < \hat{G}_{2(i)}^c$). For the drug group, $i = 1, 2, 3$ show

an improvement trend, while $i = 4$ shows a deteriorating trend although the circle is small (i.e., the proportion of observed frequencies comprising $\hat{G}_{1(4)}^c$ and $\hat{G}_{2(4)}^c$ is small relative to the total). These results imply that there might be differences in treatment effects between i levels.

Table 7: Estimates of the measure, approximate standard error, and approximate 95% confidence intervals applied to the data in Table 1.

Applied data	Estimated measure	Standard error	Confidence interval
Table 1(a)	0.308	0.078	(0.156, 0.460)
Table 1(b)	0.511	0.059	(0.395, 0.627)

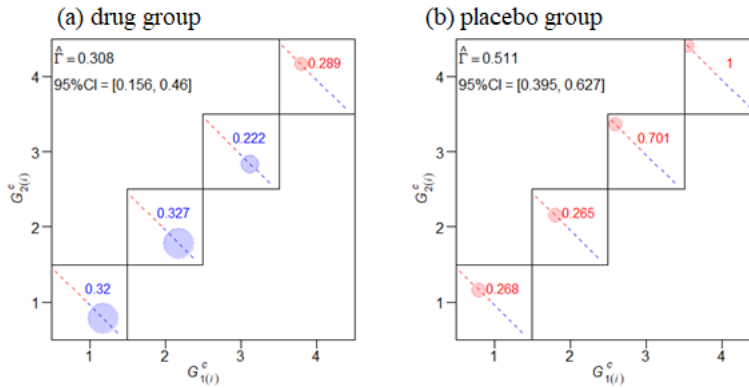


Figure 7: Visualization results of Table 1.

5. Discussion

In the proposed measure, sub-measures are used in the visualization to capture features overlooked by a single summary measure. Previous studies have adopted similar approaches, except that the sub-measures are not used for interpretation (Tomizawa *et al.*, 2003; Yamamoto *et al.*, 2011). This study demonstrates that sub-measures allow two kinds of marginal inhomogeneities to be visualized, providing a more detailed interpretation of the single-summary-measure.

The proposed visualization is analyzed using Table 1. First, because the Matusita distance satisfies the distance postulates, the visualization that draws points on two-dimensional coordinates can give a natural and intuitive interpretation. In particular, the values of existing measures based on the power-divergence (Kullback-Leibler divergence) that do not satisfy distance postulate (ii) would give different values if the distance from the start point to the end point is swapped. That is, the data in Table 1 would create two visualization patterns. In contrast, for the Matusita distance, the same value is obtained even if the distance from the start point to the end point is swapped. Hence, a special annotation is unnecessary for a visual interpretation.

Furthermore, the point in Figure 7(a) where $i = 1, 2, 3$ and $i = 4$ show different directions is difficult to discern using the existing measure proposed by Yamamoto *et al.* (2011) because it is a single-summary-measure. However, the different directions can be considered intuitively through visualization by level i . The proposed visualization does not draw the points on one coordinate because the degree of departure from MH is likely the same for each level in real data analysis (Figure 7). This is because identifying which level i of points is drawn is difficult. Hence, it is important to satisfy the distance postulates and to consider methods for visualizing categorical data of square contingency tables.

The visualization program was implemented in the R programming language (R Core Team, 2023). Noting that a graphical layout in package “ggplot2” is defined by “gtable” (and also “grid”). In addition, the arrangement of multiple figure objects can be set by package “gridExtra”. We used “grid” and “gridExtra” packages for visualization purposes. We referenced the function “agreementplot()” by the “vcd” package, which is the categorical data visualization package for the “observer agreement chart”.

6. Conclusion

The proposed measure Γ is the weighted sum of the sub-measures that

satisfy all three distance postulates. Here, we demonstrate the approximated confidence interval for Γ . The proposed visualization using the Matusita distance provides a natural visual interpretation of MH in a square contingency table. In addition, we show that the visualization can provide useful interpretations using an example.

References

- Agresti, A. (2013). *Categorical Data Analysis*, 3rd edition. Wiley, Hoboken, New Jersey.
- Ando, S., Noguchi, T., Ishii, A. and Tomizawa, S. (2021). A two-dimensional index for marginal homogeneity in ordinal square contingency tables . *SUT Journal of Mathematics* **57**, 211–224.
- Bangdiwala, S.I. (1985). A graphical test for observer agreement. *Proceeding of the International Statistics Institute* **1**, 307–308.
- Bangdiwala, S.I. (1987). Using SAS software graphical procedures for the observer agreement chart. *Proceedings of the SAS User's Group International Conference* **12**, 1083–1088.
- Berger, J.O. (1985). *Statistical Decision Theory and Bayesian Analysis*, 2nd edition. Springer, New York.
- Bishop, Y.M.M., Fienberg, S.E. and Holland, P.W. (1975). *Discrete Multivariate Analysis: Theory and Practice*. The MIT Press, Cambridge, Massachusetts.
- Blasius, J. and Greenacre, M. (1998). *Visualization of Categorical Data*. Academic Press, San Diego, California.
- Cressie, N. and Read, T.R.C. (1984). Multinomial goodness-of-fit tests. *Journal of the Royal Statistical Society, Series B* **46**, 440–464.
- Fienberg, S.E. (1975). Perspective Canada as a social report. *Social Indicators Research* **2**, 153–174.
- Friendly, M. (1994). A fourfold display for 2 by 2 by k tables. Technical Report 217, York University, Psychology Department.
- Friendly, M. (1995). Conceptual and visual models for categorical data. *The American Statistician* **49**, 153–160.

- Friendly, M. and Meyer, D. (2015). *Discrete Data Analysis with R: Visualization and Modeling Techniques for Categorical and Count Data*. CRC Press, Boca Raton, Florida.
- Haldane, J.B.S. (1932). A Note on Inverse Probability. *Mathematical Proceedings of the Cambridge Philosophical Society* **28**, 55–61.
- Hartigan, J.A. and Kleiner, B. (1981). Mosaics for contingency tables. *Computer Science and Statistics: Proceedings of the 13th Symposium on the Interface*, 268–273.
- Hartigan, J.A. and Kleiner, B. (1984). A mosaic of television ratings. *The American Statistician* **38**, 32–35.
- Kateri, M. (2014). *Contingency Table Analysis: Methods and Implementation Using R*. Birkhäuser/Springer, New York.
- Matusita, K. (1954). On the estimation by the minimum distance method. *Annals of the Institute of Statistical Mathematics* **5**, 59–65.
- Matusita, K. (1955). Decision rules based on the distance, for problems of fit, two samples, and estimation. *Annals of the Institute of Statistical Mathematics* **26**, 631–640.
- R Core Team (2023). R: A language and environment for statistical computing. R Foundation for Statistical Computing, Vienna, Austria. URL: <https://www.R-project.org/>
- Read, T.R.C. and Cressie, N. (1988). *Goodness-of-Fit Statistics for Discrete Multivariate Data*. Springer, New York.
- Riedwyl, H. and Schüpbach, M. (1983). Siebdiagramme: Graphische Darstellung von Kontingenztafeln. Technical Report 12, Institute for Mathematical Statistics. University of Bern, Bern, Switzerland.

Riedwyl, H. and Schüpbach, M. (1994). Parquet Diagram to Plot Contingency Tables. In F. Faulbaum, ed., *Softstat '93: Advances in Statistical Software*, 293–99. New York: Gustav Fischer.

Sugano, K., Kinoshita, Y., Miwa, H. and Takeuchi, T. (2012). Randomised clinical trial: esomeprazole for the prevention of nonsteroidal anti-inflammatory drug-related peptic ulcers in Japanese patients. *Alimentary Pharmacology and Therapeutics* **36**, 115–125.

Stuart, A. (1955). A test for homogeneity of the marginal distributions in a two-way classification. *Biometrika* **42**, 412–416.

Tomizawa, S. (1995). Measures of departure from marginal homogeneity for contingency tables with nominal categories. *Journal of the Royal Statistical Society, Series D* **44**, 425–439.

Tomizawa, S., Miyamoto, N. and Ashihara, N. (2003). Measure of departure from marginal homogeneity for square contingency tables having ordered categories. *Behaviormetrika* **30**, 173–193.

Yamamoto, K., Ando, S. and Tomizawa, S. (2011). A measure of departure from average marginal homogeneity for square contingency tables with ordered categories. *Revstat* **9**, 115–126.

Appendix 1

Assuming that $\{G_{1(i)} + G_{2(i)} \neq 0\}$, the power-divergence-type measure representing the degree of departure from MH proposed by Tomizawa, Miyamoto and Ashihara (2003) for $\lambda > -1$ is given as

$$\Phi^{(\lambda)} = \frac{\lambda(\lambda + 1)}{2^\lambda - 1} \sum_{i=1}^{r-1} (G_{1(i)}^* + G_{2(i)}^*) \times I_i^{(\lambda)} \left(\{G_{1(i)}^c, G_{2(i)}^c\}; \left\{ \frac{1}{2}, \frac{1}{2} \right\} \right),$$

where

$$I_i^{(\lambda)}(\cdot, \cdot) = \frac{1}{\lambda(\lambda + 1)} \left[G_{1(i)}^c \left\{ \left(\frac{G_{1(i)}^c}{1/2} \right)^\lambda - 1 \right\} + G_{2(i)}^c \left\{ \left(\frac{G_{2(i)}^c}{1/2} \right)^\lambda - 1 \right\} \right],$$

and the value at $\lambda = 0$ is taken to the limit as $\lambda \rightarrow 0$. Note that $I_i^{(\lambda)}(\cdot, \cdot)$ is the power-divergence between two distributions (see Cressie and Read, 1984; Read and Cressie, 1988, p.15). Namely,

$$I_i^{(0)}(\cdot, \cdot) = G_{1(i)}^c \log \left(\frac{G_{1(i)}^c}{1/2} \right) + G_{2(i)}^c \log \left(\frac{G_{2(i)}^c}{1/2} \right).$$

This measure has the following characteristics:

- (i) $\Phi^{(\lambda)} = 0$ if and only if the MH model holds
- (ii) $\Phi^{(\lambda)} = 1$ if and only if the degree of departure from MH is a maximum, in the sense that $G_{1(i)}^c = 1$ (then $G_{2(i)}^c = 0$) or $G_{1(i)}^c = 0$ (then $G_{2(i)}^c = 1$), for $i = 1, \dots, r - 1$

Second, assuming that $\{G_{1(i)} + G_{2(i)} \neq 0\}$, the measure representing two kinds of marginal inhomogeneities proposed by Yamamoto, Ando and Tomizawa (2011) is given as

$$\Psi = \frac{4}{\pi} \sum_{i=1}^{r-1} (G_{1(i)}^* + G_{2(i)}^*) \left(\theta_i - \frac{\pi}{4} \right),$$

where

$$\theta_i = \cos^{-1} \left(\frac{G_{1(i)}}{\sqrt{G_{1(i)}^2 + G_{2(i)}^2}} \right).$$

This measure has the following characteristics:

- (i) $\Psi = -1$ if and only if there is a structure of maximum upper-marginal inhomogeneity
- (ii) $\Psi = 1$ if and only if there is a structure of maximum lower-marginal inhomogeneity
- (iii) If the MH model holds then $\Psi = 0$, but the converse does not hold

Yamamoto *et al.* (2011) defined this structure ($\Psi = 0$) as the average MH model.

Third, assuming that $\{G_{1(i)} + G_{2(i)} \neq 0\}$, the two-dimensional measure that can simultaneously analyze the degree and directionality of departure from MH proposed by Ando, Noguchi, Ishii and Tomizawa (2021) is given as

$$\boldsymbol{\tau} = \begin{pmatrix} \Phi^{(0)} \\ \Psi \end{pmatrix}.$$

This two-dimensional measure has the following characteristics:

- (i) $\boldsymbol{\tau} = (0, 0)^t$ if and only if the MH model holds
- (ii) $\boldsymbol{\tau} = (1, -1)^t$ if and only if there is a structure of maximum upper-marginal inhomogeneity
- (iii) $\boldsymbol{\tau} = (1, 1)^t$ if and only if there is a structure of maximum lower-marginal inhomogeneity

Appendix 2

Using the delta method, $\sqrt{n}(\hat{\Gamma} - \Gamma)$ has an asymptotic variance $\sigma^2[\Gamma]$, which is given as

$$\sigma^2[\Gamma] = \sum_{k=1}^{r-1} \sum_{l=k+1}^r (p_{kl}D_{kl}^2 + p_{lk}D_{lk}^2),$$

where

$$D_{kl} = \frac{1}{\Delta} \sqrt{\frac{2 + \sqrt{2}}{2}} \sum_{i=1}^{r-1} I(k \leq i, l \geq i + 1) A_i - \frac{(l - k)}{\Delta} \Gamma,$$

$$D_{lk} = \frac{1}{\Delta} \sqrt{\frac{2 + \sqrt{2}}{2}} \sum_{i=1}^{r-1} I(k \leq i, l \geq i + 1) B_i - \frac{(l - k)}{\Delta} \Gamma,$$

$$A_i = \frac{1}{2\sqrt{C_i}} \left(2C_i + v_{1(i)} \frac{G_{2(i)}^c}{\sqrt{G_{1(i)}^c}} - v_{2(i)} \sqrt{G_{2(i)}^c} \right),$$

$$B_i = \frac{1}{2\sqrt{C_i}} \left(2C_i - v_{1(i)} \sqrt{G_{1(i)}^c} + v_{2(i)} \frac{G_{1(i)}^c}{\sqrt{G_{2(i)}^c}} \right),$$

$$C_i = v_{1(i)}^2 + v_{2(i)}^2,$$

and $I(\cdot)$ is indicator function.